Location and Dynamics of Ionophore A23187 Bound to Unilamellar Vesicles of Dimyristoylphosphatidylcholine†

Raymond F. Kauffman,‡ Clifford J. Chapman, and Douglas R. Pfeiffer*

ABSTRACT: The acid and anionic forms of ionophore A23187 bind to unilamellar vesicles of dimyristoylphosphatidylcholine with association constants of 9.40×10^4 and 6.16×10^3, respectively, at 35 °C. van't Hoff plots of binding constants for the anionic form are linear over the temperature range 4–45 °C. Analogous data for the free acid form show a discontinuity centered at the phase transition temperature of the vesicle membranes. The binding of both forms of the ionophore is entropically driven. Seven phospholipid molecules constitute an apparent binding site for the anionic form above the phase transition temperature. The apparent binding stoichiometry of the acid form is the same as for the carboxylate anion above the phase transition temperature but is increased to 12–13 phospholipid molecules per site when the membrane is in the gel state. The collisional quenching agents I^- and *N*-methylnicotinamide reduce the fluorescence of acid and anionic forms of the ionophore, respectively, regardless of whether the compound is in solution or bound to vesicles. Fluorescence lifetime, polarization, and differential polarized phase lifetime measurements show that polarization differences between the bound acid and anionic forms and polarization differences associated with the membrane phase transition arise predominantly from changes in the static rather than the dynamic components of the steady-state values. Limiting anisotropies of 1,6-diphenyl-1,3,5-hexatriene and the free acid form of A23187 are related to steady-state anisotropies in a similar manner. However, 1,6-diphenylhexatriene experiences more order within the bilayer than does A23187. The anionic form of the ionophore is more hindered in rotational motions than is the free acid. The data indicate that the benzoxazole chromophore of the bound ionophore is located at the membrane–water interface in either protonation state. Other molecular regions may extend into the bilayer for the acid but not the anionic form.

Studies on the mechanism and specificity of cation transport by ionophores have traditionally focused on interactions between the cation and the carrier [see Taylor et al. (1982) for review]. Relatively less attention has been devoted to ionophore–membrane interactions and the role these may play in establishing the transport properties of the compounds. The limited amount of information in this area has been reviewed by Painter & Pressman (1982). Ionophore A23187 is well suited for investigations of this type. The fluorescence and other spectral properties of the compound are sensitive indicators of its environment and chemical state (Kauffman et al., 1982). In the present study we have exploited these properties to reveal some aspects of how A23187 interacts with vesicle membranes prepared from dimyristoylphosphatidylcholine. The data obtained are contrasted for the acid (HA)[1] and anion (A^-) forms of the compound. Aspects of these findings have appeared previously in abstract form (Kauffman & Pfeiffer, 1981).

Materials and Methods

L-α-Dimyristoylphosphatidylcholine (DMPC) was obtained from Sigma Chemical Co. An unidentified spectral impurity (λ_{max} 258 nm) and potentially contaminating free fatty acid were removed by precipitation of the phospholipid in acetone–chloroform (9:1 v/v). The purified DMPC migrated as a single spot when analyzed by thin-layer chromatography (chloroform–methanol–water, 65:25:4 v/v/v; silica gel H). The free fatty acid content of the purified phospholipid was determined as described before (Kauffman et al., 1982) and found to be <0.0005 mole ratio. The free acid of A23187 was a gift from Robert Hamill, Eli Lilly Co. 1,6-Diphenyl-1,3,5-hexatriene (DPH) was obtained from Sigma. Tetraethylammonium perchlorate (Eastman Chemicals) was recrystallized 4 times from hot water before use. Reagent grade perchloric acid (Fisher Scientific), tetraethylammonium iodide, and tetraethylammonium hydroxide (Eastman Chemicals) were used without further purification. Distilled, deionized water and acid-washed glassware (sulfuric–nitric, 3:1 v/v) were used throughout.

Small, unilamellar vesicles of DMPC were prepared by sonication with the cup horn apparatus (Heat Systems No. 431A) as described previously (Kauffman et al., 1982). The aqueous solutions contained 33 mM tetraethylammonium perchlorate, 5 mM each of β,β-dimethylglutaric acid, Hepes, and Ches, 0.1 mM EDTA, and 0.1 mM EGTA. The aqueous phase pH extremes necessary to generate the free acid or carboxylate anion of A23187 bound to the DMPC vesicles (5.4–5.5 for HA and 10.5–10.8 for A^-) were determined and reported previously (Kauffman et al., 1982). The pH of the vesicle suspension was adjusted by the addition of $HClO_4$ or tetraethylammonium hydroxide and was monitored with a combination glass electrode (Beckman 39030) previously calibrated with standard buffers (Fisher Scientific). The nominal concentratioin of DMPC in the vesicle suspension was

† From the Hormel Institute, University of Minnesota, Austin, Minnesota 55912. *Received January 20, 1983.* This research was supported by U.S. Public Health Service Grant GM-24701 from the National Institute of General Medical Sciences, by U.S. Public Health Service Grant HL-08214 from the Program Projects Branch, Extramural Programs, National Heart, Lung and Blood Institute, by Grant 8631 from the Research Corporation, and by the Hormel Foundation.

‡ Present address: The Lilly Research Laboratories, Indianapolis, IN 46285.

[1] Abbreviations: Hepes, *N*-(2-hydroxyethyl)piperazine-*N*′-2-ethanesulfonic acid; Ches, 2-(*N*-cyclohexylamino)ethanesulfonic acid; DMPC, L-α-dimyristoylphosphatidylcholine; DPH, 1,6-diphenyl-1,3,5-hexatriene; HA, the free acid of A23187; A^-, the carboxylate anion of A23187; T_c, the gel to liquid phase transition temperature; EDTA, ethylenediaminetetraacetic acid; EGTA, ethylene glycol bis(β-aminoethyl ether)-*N*,*N*,*N*′,*N*′-tetraacetic acid.

0006-2960/83/0422-3985$01.50/0

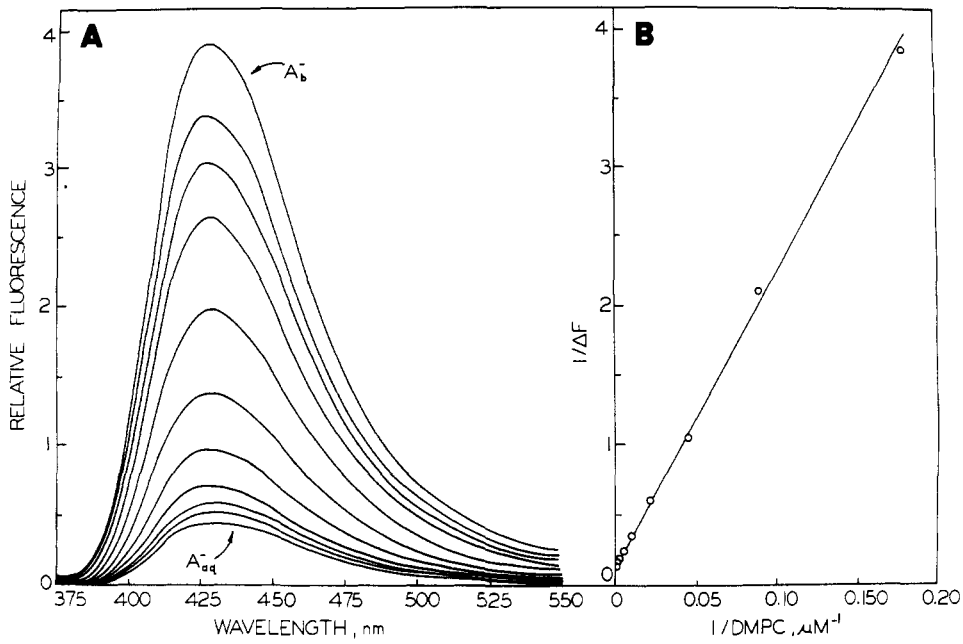

FIGURE 1: Fluorometric titration of A^- binding to unilamellar DMPC vesicles at 35 °C. Fluorescence emission spectra were obtained as described under Materials and Methods. The binding studies were carried out in aqueous solutions containing 33 mM tetraethylammonium perchlorate, 5 mM Ches, 5 mM Hepes, 5 mM β,β-dimethylglutaric acid, 0.1 mM each of EDTA and EGTA, and 2.5 μM A23187. The pH was adjusted to 10.0 with tetraethylammonium hydroxide. The solution was irradiated at 359 nm, the wavelength of maximum fluorescence excitation, with the slits set at 4 nm. (A) The corrected emission spectra for A^- were taken in the presence of increasing concentrations of DMPC vesicles ranging from 0 (A_{aq}^-) to 3.0 mM (A_b^-) lipid phosphorus. (B) The reciprocal of the increase in fluorescence at 427 nm, $1/\Delta F$, is plotted vs. the reciprocal of the total concentration of DMPC in the vesicle suspension.

determined by measurement of lipid phosphorus (Bartlett, 1959).

A23187 was added to liposomal suspensions as the free acid in ethanol. The final ethanol concentration was kept at less than 0.1 vol %, a concentration region in which this solvent does not perturb lecithin vesicles (Jain & Wu, 1977).

Steady-state fluorescence emission was measured with an SLM 8000 DS spectrofluorometer operated in the ratiometric, photon counting mode. This instrument was interfaced to an IMSAI 8080 microcomputer with dual disk drive for data manipulation and storage. Technical spectra were corrected for variations in photomultiplier sensitivity as a function of wavelength by utilizing factors obtained with a standard tungsten lamp.

Steady-state polarization (P) and anisotropy (r) values were obtained with the same fluorometer operated in the "T-format". For these studies, the fluorescence emission was isolated from Rayleigh and Raman scattering by use of Schott KV418 filters. Polarization values in the absence of Brownian motion (P_0) were determined at −24 °C with frozen solutions of glycerol or 90 wt % glycerol for HA and A^-, respectively. The glycerol was treated with Chelex to remove contaminating divalent cations, and the apparent pH of the 90 wt % solution was adjusted to 10.8 with tetraethylammonium hydroxide to generate A^-.

Fluorescence lifetimes (τ) were determined by the phase modulation method of Spencer & Weber (1969) by utilizing an SLM 4800 subnanosecond spectrofluorometer. Filters were used as described above to isolate the fluorescence emission from scattered light. Fluorescence lifetimes were measured with the polarizer in the emission path oriented to 54.7° to eliminate effects on τ due to Brownian rotation (Spencer & Weber, 1970). A solution of 1,4-bis(5-phenyloxazol-2-yl)-benzene (POPOP) was used as a reference lifetime standard (τ_{POPOP} = 1.35 ns in ethanol; F. G. Prendergast, personal communication). When the data indicated the presence of more than one fluorescent species, individual lifetimes were resolved by the method of Weber (1981) by assuming two fluorescent components in the system.

Differential phase lifetimes were determined by the method originally described by Mantulin & Weber (1977) as modified by Lakowicz & Prendergast (1978). Calculations of differential tangents, hindered rotational relaxation rates (R), and limiting hindered anisotropy (r_∞) were performed as described by Lakowicz et al. (1979).

Results

Binding of A23187 to Unilamellar DMPC Vesicles. The fluorometric titration of A^- with DMPC vesicles at 35 °C is shown in Figure 1A. The enhancement of fluorescence emission that occurs at increasing concentrations of vesicles is taken to indicate association of the ionophore with the DMPC bilayer (Puskin et al., 1981; Kolber & Haynes, 1981). A straight line is obtained when the reciprocal of the fluorescence enhancement (ΔF) at the wavelength of maximal emission (427 nm) is plotted against the reciprocal of the nominal DMPC concentration (Figure 1B). This latter observation reveals that binding of the ionophore to the vesicles can be represented by the equation

$$A^- + \text{DMPC} \overset{K_b}{\rightleftharpoons} A_b^- \qquad (1)$$

where A^- represents the anion of A23187 in aqueous solution, A_b^- is the membrane-bound ionophore, DMPC is the phospholipid in the vesicle suspension, and K_b is the apparent equilibrium binding constant as defined by

$$K_b = [A_b^-]/([\text{DMPC}][A^-]) \qquad (2)$$

In eq 2 $[A_b^-]$ and [DMPC] are nominal concentrations (i.e., number of moles per liter of vesicle suspension). The linearity of the double-reciprocal plot implies that the concentration of free DMPC is approximately equal to the total DMPC (i.e., the free DMPC is in great excess over the concentration of A_b^-); consequently, the equilibrium binding constant can be

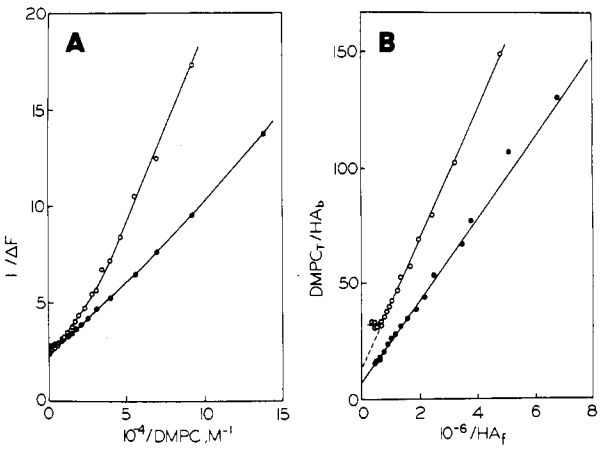

FIGURE 2: Fluorometric titration of HA binding to unilamellar DMPC vesicles at 35 °C. Fluorescence was monitored at excitation and emission wavelengths of 380 and 435 nm, respectively. The composition of the solution was identical with that described in Figure 1, except that the pH was adjusted to 4.0 with perchloric acid. (A) The reciprocal of the increase in fluorescence seen upon vesicle addition is plotted vs. the reciprocal of the DMPC concentration at 15 (○) and 35 °C (●). (B) The fluorescence data from panel A at 15 (○) and 35 °C (●) are replotted according to eq 3 from the text. The bound and free states of HA are referred to as HA_b and HA_f, respectively. The dashed line represents the linear extrapolation of the 15 °C data back to the y axis. The y intercepts are 12.7 and 6.9 at 15 and 35 °C, respectively.

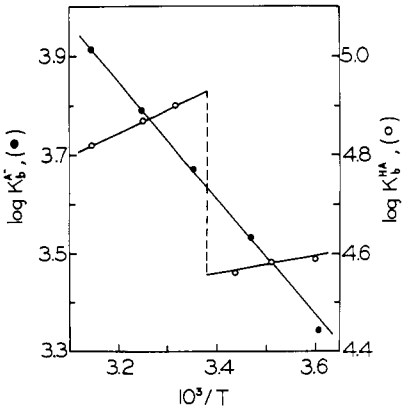

FIGURE 3: van't Hoff plot for the binding of the free acid and anion of A23187 to unilamellar DMPC vesicles. Binding constants for the free acid [K_b^{HA} (○)] and anion [$K_b^{A^-}$ (●)] of A23187 were determined as described in Figures 1 and 2 at various temperatures. The logarithms of the binding constants are plotted vs. the reciprocals of the absolute temperatures. The discontinuity in the curve for HA (dashed line) is drawn at the phase transition temperature for DMPC vesicles (23 °C).

Table I: Thermodynamic Parameters for the Binding of the Free Acid and Anion of A23187 to Unilamellar DMPC Vesicles[a]

	ΔG (kcal/mol)	ΔH (kcal/mol)	ΔS [cal/(mol·deg)]
HA	−6.8	−2.1	15
A^-	−5.3	5.4	35

[a] Free energy (ΔG), enthalpy (ΔH), and entropy (ΔS) were obtained from the van't Hoff plot for the binding of A23187 to DMPC vesicles (Figure 3). In the case of HA, the thermodynamic parameters were calculated from the data obtained at temperatures above T_c (23 °C).

calculated from the ratio of the intercept to the slope from the double-reciprocal plot in Figure 1B. For the data shown in Figure 1, K_b is equal to 6.16×10^3 M.

To determine the stoichiometry of A^- binding to the membrane, the data were plotted according to the equation

$$[DMPC_T]/[A_b] = 1/(K_b[A^-]) + \eta \quad (3)$$

where $DMPC_T$ is the total concentration of the phospholipid and η is the number of phospholipid molecules per bound ionophore at saturation. Equation 3 is equivalent to eq 2 except that the equation for conservation of mass (eq 4) was substituted into eq 1 followed by rearrangement. The amount of A^- bound to the membrane, A_b^-, was calculated from the fluorescence data by assuming that the fraction bound was equal to $\Delta F/\Delta F_{max}$. The plot of $[DMPC_T]/[A_b^-]$ vs. $1/[A^-]$ yields a straight line, and the y intercept (η) indicated saturation of the membrane occurred at one molecule of A^- per seven to eight molecules of DMPC.

$$DMPC_T = DMPC + \eta A_b^- \quad (4)$$

Titrations of DMPC vesicles binding to the free acid form of the ionophore were obtained from fluorescence enhancement data at the wavelength of maximum emission for the bound compound (435 nm). Complete spectra were not recorded because a unstable, doubly protonated form of the compound exists in aqueous solutions below pH values of approximately 4 (Kauffman et al., 1982). It is therefore desirable to complete the experiments in a minimal time. The single wavelength measurements allowed completion of the titration before the decomposition reaction (half-life = 1.7 h) could significantly affect the data. In contrast to the results obtained with A^-, the double-reciprocal plots from the titrations with HA are nonlinear both above and below the phase transition temperature (Figure 2A). However, as shown in Figure 2B, the data yield a straight line when plotted according to eq 3 (substituting HA for A^-), and K_b can be obtained from the reciprocal of the slope. The value obtained at 35 °C is 9.40 $\times 10^4$ or approximately 15-fold greater than the value obtained for the A^- form. The number of phospholipid molecules per HA bound (η) is 6.9 ± 0.1 (n = 3) at 35 °C and does not vary with temperature above the T_c. At temperatures below T_c, however, the value of η increases to 12–13. The discontinuity in the 15 °C curve (Figure 2B, open circles) is apparently due to the formation of micellar aggregates of HA; i.e., the concentration of HA at which $[DMPC]/[HA_b]$ becomes constant (1.5 μM) is equal to the critical micellar concentration. Consistent with this interpretation is the observation that a substantial increase in light scattering by solutions of HA in the absence of vesicles occurs at concentrations of the compound above 1.5 μM (data not shown).

The apparent equilibrium constants for the association of HA and A^- with the membrane were determined at various temperatures encompassing T_c. The van't Hoff plot of these values for A^- is linear, whereas a discontinuity exists at T_c in the case of HA (Figure 3). Thermodynamic parameters (ΔG, ΔH, and ΔS) were calculated from the binding constants and the slopes of the van't Hoff plot; the values are presented in Table I.

Location of A23187 Associated with DMPC Vesicles. Fluorescence quenching experiments using the collisional quencher I^- were carried out to further probe the location of A23187 within the phospholipid bilayer. I^- ions are charged, highly hydrated, and effectively impermeant to phosphatidylcholine vesicles (Jendrasiak, 1972). The ability of this ion to quench the fluorescence of a membrane-bound species, therefore, can be taken to indicate the presence of the fluorophore at the aqueous interface of the outer monolayer. Stern–Volmer plots for the quenching of HA_b and HA_{aq} by I^- (Figure 4) reveal that both solution HA and membrane-bound HA are quenched by this agent. The quenching con-

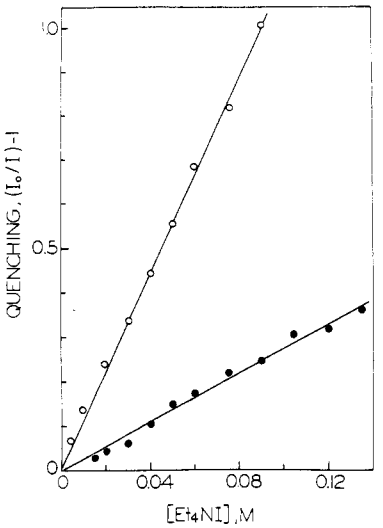

FIGURE 4: Stern–Volmer plot for the quenching of HA fluorescence by I^- at 35 °C. Fluorescence of HA was monitored as described under Materials and Methods at excitation and emission wavelengths of 380 and 435 nm, respectively. Quenching of aqueous HA (○): the aqueous solution contained 33 mM tetraethylammonium perchlorate, 5 mM Ches, 5 mM Hepes, 5 mM β,β-dimethylglutaric acid, 0.1 mM each of EDTA and EGTA, and 2.5 μM A23187. The pH was adjusted to 4.53 with perchloric acid. The concentrations of tetraethylammonium iodide present in the solutions are indicated in the figure. Quenching of membrane-bound HA (●): the conditions were identical with those described for aqueous HA except for the inclusion of DMPC vesicles at 3.0 mM lipid phosphorus. In separate control experiments tetraethylammonium chloride, at concentrations up to 120 mM, had no effect on the fluorescence of the bound species.

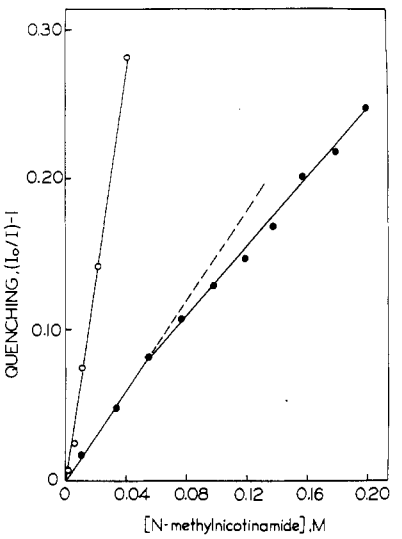

FIGURE 5: Stern–Volmer plot for the quenching of A^- fluorescence by *N*-methylnicotinamide. Experiments were performed as described in the legend to Figure 4 except that the excitation and emission wavelengths were 360 and 425 nm, respectively, the pH was adjusted to 10.7 with tetraethylammonium hydroxide, and *N*-methylnicotinamide chloride at the indicated concentrations was employed as the quenching agent. (○) Quenching of aqueous A^-. (●) Quenching of membrane-bound A^-.

stant for the bound species (i.e., slope of the Stern–Volmer plot) is only a factor of 4 lower than that of the aqueous species (2.85 M^{-1} compared to 10.9 M^{-1}, respectively). In contrast to these findings, I^- produced no detectable quenching of DPH fluorescence when this highly hydrophobic molecule was associated with the DMPC vesicles (data not shown). Membrane-associated DPH is known to be located within the hydrocarbon region and oriented parallel to the phospholipid acyl groups (Andrich & Vanderkooi, 1976).

Fluorescence of the species A^- was much less susceptible to quenching by I^- regardless of whether solution or membrane-bound ionophore was employed. This observation probably reflects a diminished collision frequency between the anionic quenching agent and the anionic benzoxazole chromophore. Both solution A^- and membrane-bound A^- are quenched by the cationic agent *N*-methylnicotinamide (Figure 5). The membrane-bound species shows evidence of heterogeneity as indicated by the biphasic nature of the Stern–Volmer plot. The quenching constants calculated from these data are 6.67 M^{-1} for aqueous A^- and 1.48 and 1.12 M^{-1} for the strongly and less strongly quenched components of the membrane-bound species, respectively. Like I^-, *N*-methylnicotinamide fails to quench the fluorescence of DPH when the probe is associated with DMPC vesicles (data not shown).

To facilitate a more detailed analysis of the quenching data and other data to be presented below, fluorescence lifetimes of A23187 were determined under conditions of interest. The results of these experiments are shown in Table II. The lifetime of A^- is 3–10-fold shorter than that of HA, as might be expected, since the fluorescence yield of A^- is less than that of HA (Kauffman et al., 1982). Two fluorescing species are present as indicated by heterogeneity in the lifetime data. A second fluorescent component which is present in aqueous solutions of HA (τ = 3.7 ns) appears to be a micellar aggregate of the ionophore. The shorter lifetime of the compound in this

Table II: Fluorescence Lifetime Data for the Free Acid (HA) and Monocarboxylate Anion (A^-) of A23187[a]

environment	temp (°C)	lifetime (ns) HA	lifetime (ns) A^-
H_2O	35	12.3[b]	1.2
90 wt % MeOH	35	9.4	2.3
$CHCl_3$	35	8.3	
DMPC vesicles	35	11.5	2.3[c]
DMPC vesicles	25	11.9	2.9[c]
DMPC vesicles	15	12.0	4.2[c]

[a] The lifetime of the fluorescence emission was measured as described under Materials and Methods. The excitation beam was modulated at 18 MHz for these measurements. All of the above solutions, except for $CHCl_3$, contained the following: 33 mM tetraethylammonium perchlorate, 5 mM Hepes, 5 mM Ches, 5 mM β,β-dimethylglutaric acid, and 0.1 mM each of EDTA and EGTA. The concentration of A23187 was 5 μM, and DMPC vesicles were employed at a concentration of 3 mM lipid phosphorus. In all cases fluorescence of the ionophore was determined at the appropriate pH and wavelength of maximum fluorescence excitation [see Kauffman et al. (1982)]. [b] Heterogeneity analysis revealed a second fluorescent component (30 fluorescence %) with τ = 3.7 ± 0.6 ns, presumably due to micellar aggregates of HA (see text). [c] Fluorescence emission due to membrane-bound A^- was heterogeneous. At 35 °C the lifetime of the second fluorescent component (approximately 10 fluorescent %) was 10.4 ± 2.4 ns.

state could be due to self-quenching of the fluorescence emission by neighboring molecules of HA in the micelle. Consistent with this interpretation is the fact that the fluorescence of an aqueous solution of HA at these concentrations increases as the temperature is raised (data not shown). This effect would be expected, due to the increase in the critical micelle concentration at higher temperatures. The lifetime of A_b^- changes nearly 2-fold in going from 15 to 35 °C whereas the value for HA_b is nearly constant over this temperature range. The change in τ for A_b^- is accompanied by a proportional change (r = 0.986) in the fluorescence yield at the emission maximum (data not shown). The lifetimes of A23187 in 90 wt % MeOH and CHCl3 are included in Table II for comparison with the values obtained in H_2O or on the membrane.

Table III: Differential Polarized Phase Fluorometric Studies of A23187 Bound to DMPC Vesicles[a]

ionophore species	environment	temp (°C)	anisotropy (r)	$\Delta\Gamma$ (ns)	log R (rad/s) Perrin equation	log R (rad/s) hindered rotations	limiting anisotropy
HA	H_2O	35	0.007				
	DMPC vesicles	15	0.194	1.16	7.10	7.69	0.144
	DMPC vesicles	23	0.128	1.43	7.43	7.77	0.070
	DMPC vesicles	35	0.085	1.28	7.69	7.94	0.037
A^-	H_2O	35	0.065				
	DMPC vesicles	15	0.271	0.244	7.15	8.02	0.234
	DMPC vesicles	23	0.249	0.326	7.38	7.93	0.178
	DMPC vesicles	35	0.220	0.334	7.64	8.02	0.128

[a] Fluorescence anisotropy and $\Delta\Gamma$ were measured by the phase modulation technique at 18 MHz as described under Materials and Methods. Depolarizing rotational rates (R) were either calculated from the Perrin equation (Perrin, 1926) or obtained from a hindered rotation model as described by Lakowicz et al. (1979). The composition of the solution and the pH values for generating HA and A^- are described in Table II.

Rotational Mobility of A23187 Associated with DMPC Vesicles. Fluorescence polarization data can also yield information about the location and mobility of a fluorophore within its environment; consequently, the polarization values for A23187 were measured at various temperatures spanning the phase transition temperature, and the data are presented in Figure 6. Also included in Figure 6 are the polarization data for membrane-bound DPH in order to show clearly the acyl chain phase transition at approximately 23 °C. The polarization of A^-_b is substantially greater than that of HA over the entire range of temperatures examined (5–40 °C). However, both species have very similar intrinsic polarization (P_0), the values determined in frozen glycerol solutions being 0.463 and 0.465 for A^- and HA, respectively. The polarization of the bound species is decreased by passing from gel to the liquid-crystalline phase with the strongest effect seen with the free acid form. In neither case is the effect as great as that observed with DPH.

Differential polarized phase fluorometry was employed to investigate the depolarizing rotations of HA and A^- bound to the DMPC vesicles. For this analysis it was assumed that A23187 undergoes isotropic depolarizing rotations within the membrane. This assumption may not be entirely valid (differential polarized lifetime analysis of A23187 in isotropic solvents suggests that this compound is an anisotropic rotator; F. G. Prendergast, personal communication); nevertheless, this analysis can yield insight into relative differences in the depolarizing rotations of HA and A^- within the membrane. The differential phase data are presented in Table III. Hindered rotational relaxation rates (R) and limiting anisotropy values (r_∞) were calculated from the steady-state anisotropy data and differential phase lifetime measurements as described by Lakowicz et al. (1979). Unhindered rotational rates obtained from the equation of Perrin (1926) are also included in Table III for comparison. The limiting anisotropy of HA_b is reminiscent of that of DPH (Lakowicz et al., 1979) in that it tended toward very low values (0.03–0.04) at temperatures above the phase transition. In contrast, r_∞ for A^-_b remained at a relatively high value (0.13) above T_c.

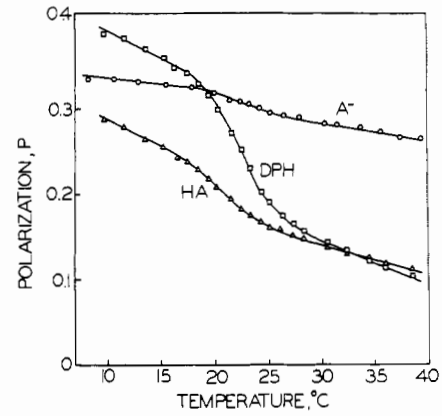

FIGURE 6: Polarization of HA, A^-, and DPH bound to unilamellar DMPC vesicles as a function of temperature. Fluorescence polarization values for the membrane-bound species were determined as described under Materials and Methods. The aqueous solutions contained 33 mM tetraethylammonium perchlorate, 5 mM Ches, 5 mM Hepes, 5 mM β,β-dimethylglutaric acid, 0.1 mM each of EDTA and EGTA, and DMPC vesicles at a concentration of 3.0 mM lipid phosphate; A23187 and DPH were present at 2.5 and 1 μM, respectively. The pH of the solutions was adjusted to 4.0 for HA and DPH or 10.8 for A^-. Essentially identical results were obtained with DPH at the higher pH. The excitation wavelengths for the individual compounds were the following: HA, 380 nm; A^-, 360 nm; DPH, 360 nm. Each data point represents the mean of at least three measurements, and the average standard deviation was 0.5%. The data are representative of results obtained in three separate experiments.

Discussion

The fluorescence properties of A23187 can be exploited to provide information about how the ionophore interacts with bilayer membranes. The affinity of the free acid form for DMPC vesicles is greater than that of A^-, as judged by the approximately 10-fold higher values of K_b for HA compared to those for A^- (Figure 3). A similar ratio of binding constants for these two species interacting with DMPC vesicles has been reported by Kolber & Haynes (1981). The overall difference in membrane affinity is consistent with the probable higher solvation energy of A^- compared to HA in the aqueous phase. However, the present data have not been corrected for the effects of surface charge on K_b. Presumably, this factor could be significant in the case of A^- binding and may also be, in part, responsible for the higher affinity of HA. The ability of the ionic strength components present in the media to mask the surface charge developed upon the binding of A^- will have to be evaluated before the effect of protonation state on K_b can be fully interpreted.

The linearity of the van't Hoff plot for A^-_b over a temperature range spanning T_c provides evidence for an interfacial location of this membrane-bound species. If portions of the molecule were located in the bilayer acyl group region, a significant effect of phase state on the apparent binding affinity would probably be observed. The apparent interfacial location of the species A^- is a useful finding since previous results on the intramembrane location of the benzoxazole chromophore, based on the spectral properties of the membrane-bound compound compared to those of the compound in solutions of methanol–water, were more ambiguous for A^- than for the

free acid form. The ΔH and ΔS values obtained from the data in Figure 3 show that the binding of A^- to the vesicles is entropically driven and that the values of these energetic terms are similar to those observed for other entropy-driven processes such as micelle formation (Corkill et al., 1964; Schick, 1963).

The van't Hoff plot for binding of HA to the vesicles reveals some striking differences between the binding characteristics of this species and those of the anion. A negative heat of binding (ΔH) is observed for HA, although the magnitude of this term is small compared to $-T\Delta S$. The association of HA with the bilayer is therefore also entropically driven. The entropy of binding for HA is less than half that of A^-. This observation is suprising in light of the expected increased hydrophobicity of HA compared to A^- and suggests that below the critical micelle concentration in water, HA still exists in a state of low aggregation (dimer etc.) rather than as a monomer.

The discontinuity at T_c in the van't Hoff plot for HA binding is in striking contrast to the linearity observed with A^-. This observation could be taken as evidence that the species HA is located substantially deeper in the bilayer than is the species A^-. Such an interpretation need not conflict with the previous finding of an interfacial location based on spectral properties and estimation of the carboxylate protonation constant (Kauffman et al., 1982), since the former parameters report only on the location of the benzoxazole chromophore in the molecule. The binding constant measurements, however, reflect the aggregate membrane interactions of all portions of the molecular structure. Thus, while all regions of the molecule must be located primarily at the interface for the species A^-, some regions distal to the benzoxazole group of HA may extend into the acyl groups of the membrane.

Further analysis shows that an alternative explanation for the discontinuity must also be considered. The binding constants presented in Figure 3 are apparent constants because the stoichiometry of binding (η) has not been taken into account. The true binding constant (K_b^t) is defined by the equation

$$K_b^t = [A_b]/([A][DMPC/\eta]) \quad (5)$$

where A and A_b are the free and bound forms of A23187 (protonation state undesignated), respectively, and $[DMPC/\eta]$ is the nominal concentration of free "binding sites" for A23187 within the vesicles. The apparent and true binding constants in eq 2 and 4 are related by the equation

$$K_b = \eta K_b \quad (6)$$

The data in Figure 2B demonstrate that η increases almost 2-fold at temperatures below T_c. Consequently, the shift in log K_b^t for the free acid (0.37 unit) at the gel to liquid transition temperature can be accounted for largely by a change in η, rather than K_b. A possible explanation for the change in η is that at temperatures below T_c only the outer half of the bilayer is accessible to HA for binding, whereas at temperatures above T_c HA can traverse the bilayer and thus associate with both halves. Since the van't Hoff plot for A^- binding is not discontinuous, the above interpretation would suggest conversely that the anion is confined to the outer monolayer in both the gel and liquid phase states and that nearly twice as many phospholipid molecules are needed to form a binding site for the species HA as for the species A^-. Unfortunately, the lower affinity of the vesicles for A^- and the entropic nature of the binding forces have so far precluded accurate estimation of η at lower temperatures. A low permeability of the species A^- is expected, however, since earlier work showed that the compound cannot act as a protonphore in mitochondria (Reed & Lardy, 1972; Pfeiffer et al., 1976). There is also no reason to doubt a priori that A^- and HA could utilize different numbers of phospholipid molecules as a binding site based on the available data. Thus, both acyl group interactions involving molecular regions distant from the fluorescent chromophore and the effect of phase state on the permeability of HA may be involved in producing the discontinuous van't Hoff plot seen in Figure 3, and further work will be necessary to fully explain this behavior.

The presence of the benzoxazole chromophore in both HA and A^- at the bilayer interface was confirmed by the quenching experiments shown in Figures 4 and 5. When collisional quenching mechanisms are assumed and the lifetime values reported in Table II are utilized, quenching rates may be calculated from the Stern–Volmer equation. In the case of HA quenching by I^-, the values are 8.7×10^8 and 2.5×10^8 $M^{-1}\cdot s^{-1}$ for the aqueous and membrane-bound species, respectively. In the case of A^- quenching by *N*-methylnicotinamide, the equivalent values are 5.6×10^9 $M^{-1}\cdot s^{-1}$ for the aqueous species and 6.4×10^8 and 4.9×10^8 $M^{-1}\cdot s^{-1}$ for the readily and the less readily quenched components of the membrane-bound species, respectively. It is difficult to interpret the significance of the absolute rates and the differences seen between the acid and anion forms of the ionophore since the two quenching agents are chemically dissimilar. Preferential interactions between the quenching agents and the chromophore may exist and may be factors in establishing the absolute quenching rates. However, comparisons between the quenching rates for aqueous and membrane-bound species are useful. Particularly in the case of HA, it appears that membrane association does not greatly hinder the approach of the quenching agent to the excited-state chromophore since the quenching rate is about 30% of the value seen than with the aqueous compound. A halving of the quenching rate upon binding to the membrane interface would be expected on simple geometrical grounds since in the bound state, any approach of the quenching agent from behind the membrane would be prevented, whereas in solution, an approach from all directions in three-dimensional space would presumably be possible. In addition, a substantial fraction of the bound ionophore should be associated with the inner monolayer and so inaccessible to extravesicular I^- from any direction, assuming that the time required for transmembrane diffusion is long compared to the fluorescence lifetime. This condition appears to be met based on reported values for the diffusion constant of HA (28/s) across bilayer membranes (Kolber & Haynes, 1981). Together these factors alone could account for the reduction in quenching rate upon membrane binding. The data thus indicate that the benzoxazole chromophore in HA is readily accessible to aqueous I^- which means a predominantly interfacial location.

Puskin et al. (1981) found that the fluorescence of membrane associated HA is quenched by Tempo stearamide and by nitroxide spin-labeled fatty acid methyl esters incorporated into vesicle membranes. The quenching efficiency was relatively independent of the spin probe location and indicated a more uniform distribution of fluorophore throughout the membrane than do the results presented here. A complete explanation for the apparent discrepancy is not obvious; however, it seems possible that the relatively bulky spin-label probes may introduce packing defects in the membrane and thereby enhance access of the ionophore to the membrane interior and the acyl group associated spin-label. In addition, quenching by the spin-label occurs through the Förster transfer mechanism and is effective over distances of approximately

10 Å (Puskin et al., 1981). These distances are relatively large compared to the membrane dimensions, thereby limiting the ability of the probes to resolve the different locations.

In the case of A^- quenching by *N*-methylnicotinamide, membrane association reduces the quenching rate by approximately 10-fold, regardless of whether the readily or less readily quenched membrane-bound fraction is considered. The magnitude of that change is greater than can be accounted for solely by geometrical arguments. However, we doubt that the larger effect means that a greater component of membrane-associated A^- is located in the bilayer interior than is the case with membrane-associated HA. Such an interpretation would conflict with the data in Figure 3 and would be contrary to the expected effect of the negative charge born by A^-. A more reasonable explanation is that the approach of the relatively bulky *N*-methylnicotinamide cation to the excited-state chromophore is more hindered by the atoms comprising to phospholipid head-group structures than in the case of the relatively small I^-. More hindered motions of the benzoxazole chromophore in membrane-bound A^- compared to HA (see below) may also contribute to diminished collision rates between A^- and the quenching agent.

The measurements of fluorescence polarization and differential polarized phase lifetimes were carried out to examine the dynamics of A23187 within the membrane environment. The classical approach in studies of this type has been to calculate rotational rates of membrane-bound species from steady-state polarization (or anisotropy) values and fluorescence lifetimes by utilizing the Perrin equation (1926). These methods assume that the fluorophore is spherically shaped and in an environment which allows isotropic rotations. Information of this type is available for free and complexed A23187 bound to the membranes of mitochondria and sarcoplasmic reticulum (Case et al., 1974).

More recently, time-resolved fluorescence anisotropy decay measurements [for a review, see Van Blitterswijk et al. (1981)] and differential polarized phase lifetime measurements (Lakowicz et al., 1979) have revealed that steady-state anisotropy values for membrane-bound probes, in particular DPH and charged analogues of DPH, can be resolved into a dynamic component, r (dependent upon the rate of depolarizing rotations), and a static component, r_∞ (dependent upon the degree to which fluorophore rotations are hindered by molecular packing of the lipids). These studies have shown that in membranes, steady-state polarization (or anisotropy) is largely determined by the static component, r_∞. The results have emphasized that the bilayer interior cannot be considered to be an isotropic medium, especially at temperatures below T_c where r_∞ is large. Consequently, measurements of steady-state polarization alone cannot yield quantitatively meaningful rotational rates.

The hindered rotational rates and limiting anisotropy for HA and A^- bound to DMPC vesicles (Table III) show that, as with DPH, r_∞ is a significant component of the steady-state anisotropy. The hindered rotational rate of bound HA is increased by less than a factor of 2 upon passage from the gel to liquid-crystalline state, whereas this parameter is essentially unchanged by the phase transition in the case of bound A^-. The hindered rotational rates of the two protonation states are also closely similar, particularly above T_c. Thus, differences in polarization between the bound acid and anion and changes in polarization associated with the phase transition (Figure 6) reflect predominantly differences in r_∞. In this respect, the dynamics of the membrane-associated ionophore are like those of DPH and related compounds. Describing the depolarizing motions of the bound ionophore and the changes in these motions which are reflected by changes in r_∞ is more difficult for the ionophore than for DPH. With the latter molecule, the excitation and emission vectors are oriented parallel to the long axis of the molecule which, together with the orientation of that axis with respect to the acyl chains, has allowed a relatively detailed description of the motions involved [see Engel & Prendergast (1981) and references therein]. With A23187, fluorescence depolarization presumably can reflect motions of the entire molecule as well as rotation of the substituted benzoxazole around the hinge region bonds which link the chromophore to the spiroketal portion of the molecule (Deber & Pfeiffer, 1976). Thus, changes in the hindered rotational rate or limiting anisotropy of the bound ionophore can reflect changes in either the molecular or the intramolecular environment. In addition, with the information at hand, the possibility that the bound ionophore can exchange to a significant extent with the aqueous pool during the lifetime of the excited state cannot be ruled out. Thus, it is possible, although unlikely, that a degree of depolarization occurs by rotation of molecules in the aqueous phase.

With the above complexities in mind, it is interesting to note that for DPH, an empirical relation between steady-state anisotropy (r) and r_∞ has been found (Van Blitterswijk et al., 1981) that is applicable to a wide variety of membranes and agrees well with predictions based on a theory of rotational dynamics in liquid crystals (Nordio & Segre, 1979). By use of this relationship [$r_\infty = {}^4/_3(r_s) - 0.10$; $0.13 < r_s < 0.28$], the calculated values for HA_b are 0.159, 0.071, and 0.030 at 15, 25, and 35 °C, respectively. Analogous values for A_b^- are 0.260, 0.232, and 0.193. Comparing these predicted values of r_∞ to those observed (Table III) shows good agreement for HA but not A^-. The parameter r_∞ is related to an orientational order parameter, S, of the lipid bilayer according to the equation

$$S^2 = r_\infty/r_0 \qquad 0 \le S \le 1 \tag{7}$$

where r_0 is the anisotropy in the absence of Brownian motion (Heyn, 1979; Jahnig, 1979; Lipari & Szabo, 1980). Since r_0 is nearly the same for HA and DPH ($\sim$0.4), a given value of r for bound HA appears to report the same structural order for the bilayer as does an equivalent r value for DPH. Since the polarization of HA is less than that of DPH below phase transition temperature (Figure 6), HA evidently experiences less order within the membrane at a given temperature. This finding is consistent with a predominantly interfacial location for the chromophore in HA where that moiety would be less subject to ordering constraints imposed by the acyl chains, thereby giving rise to higher values of r_∞. However, the fact that an empirical relationship based on the properties of an acyl group region probe such as DPH appears to describe motional constraints experienced by bound HA better than bound A^- must be taken, together with Figure 3, as evidence that some portions of the protonated molecule penetrate the hydrocarbon region.

The higher values of r_∞ observed for membrane-bound A^- compared to HA also deserve further comment. Since the chromophore is located primarily at the interface with both A^- and HA, a plausible explanation for the effect of protonation state on r_∞ is that fewer degrees of rotational freedom are available to the anion compared to the acid. Several factors may contribute to motional constraint on the anion. Deprotonation could tend to promote hydrogen bonding between the carboxylate group and keto pyrole moiety as observed in the crystalline state (Chaney et al., 1974) and in chloroform solutions (Deber & Pfeiffer, 1976). This would produce con-

formational changes which could alter the rotational freedom of the bound molecule and could diminish intramolecular motion of the chromophore. An increased tendency of the ionophore to interact with the quaternary nitrogen in the choline group would also be expected upon ionization. This interaction could also restrict both molecular and intramolecular motions, thereby increasing r_∞. However, the dominant effect of ionization on motional freedom probably arises simply from the resulting increase in amphiphilic character. The hydration energy of the carboxylate anion should place a degree of constraint on the modes of depolarizing rotations available, since any rotation in which the carboxylate group is brought into the bilayer interior is not likely to occur. The increase in r_∞ which accompanies ionization of HA is reminiscent of the results of Prendergast et al. (1981) on a charged derivative of DPH: 1-[4-(trimethylammonio)phenyl]-6-phenyl-1,3,5-hexatriene (TMA-DPH). In this compound, a cationic group (trimethylammonio group) is affixed to the para position of one phenyl moiety of DPH. The compound, considered by the authors to be anchored at the interface, also exhibited relatively high values of r_∞ (0.12–0.14) at temperatures above T_c in lecithin vesicles. These findings support a significant role for charge-derived anchoring of A^- at the interface in establishing a high value of r_∞.

Acknowledgments

We express our appreciation to Drs. Gregory D. Reinhart and Frank G. Prendergast for the use of fluorescence instrumentation at the Mayo Clinic, Rochester, MN, and for many helpful discussions of the data. Helpful discussions with Dr. Howard L. Brockman of the Hormel Institute are also acknowledged.

Registry No. HA, 52665-69-7; DMPC, 18194-24-6.

References

Andrich, M. P., & Vanderkooi, J. M. (1976) *Biochemistry 15*, 1257–1261.

Bartlett, G. R. (1959) *J. Biol. Chem. 234*, 466–468.

Case, G. D., Vanderkooi, J. M., & Scarpa, A. (1974) *Arch. Biochem. Biophys. 162*, 174–185.

Chaney, M. O., DeMarco, P. V., Jones, N. D., & Occolowitz, J. L. (1974) *J. Am. Chem. Soc. 96*, 1932–1933.

Corkill, J. M., Goodman, J. F., & Tate, J. R. (1964) *Trans. Faraday Soc. 60*, 996–1002.

Deber, C. M., & Pfeiffer, D. R. (1976) *Biochemistry 15*, 132–141.

Engel, L. W., & Prendergast, F. G. (1981) *Biochemistry 20*, 7338–7345.

Heyn, M. P. (1979) *FEBS Lett. 108*, 359–364.

Jahnig, F. (1979) *Proc. Natl. Acad. Sci. U.S.A. 76*, 6361–6365.

Jain, M. K., & Wu, N. M. (1977) *J. Membr. Biol. 34*, 157–201.

Jendrasiak, G. L. (1972) *Chem. Phys. Lipids 9*, 133–146.

Kauffman, R. F., & Pfeiffer, D. R. (1981) *Fed Proc., Fed. Am. Soc. Exp. Biol. 40*, 1772 (Abstr. No. 1334).

Kauffman, R. F., Taylor, R. W., & Pfeiffer, D. R. (1982) *Biochemistry 21*, 2426–2435.

Kolber, M. A., & Haynes, D. H. (1981) *Biophys. J. 36*, 369–391.

Lakowicz, J. R., & Prendergast, F. G. (1978) *Science (Washington, D.C.) 200*, 1399–1401.

Lakowicz, J. R., Prendergast, F. G., & Hogen, D. (1979) *Biochemistry 18*, 508–519.

Lipari, G., & Szabo, A. (1980) *Biophys. J. 30*, 489–506.

Mantulin, W. W., & Weber, G. (1977) *J. Chem. Phys. 66*, 4092–4099.

Nordio, P. L., & Segre, U. (1979) in *Mol. Phys. Liq. Cryst. Lect. NATO Adv. Study Inst., 1977*, 411–426.

Painter, G. R., & Pressman, B. C. (1982) *Top. Curr. Chem. 101*, 83–110.

Perrin, F. (1926) *J. Phys. Radium 7*, 390–401.

Pfeiffer, D. R., Hutson, S. M., Kauffman, R. F., & Lardy, H. A. (1976) *Biochemistry 15*, 2690–2697.

Prendergast, F. G., Haughland, R. P., & Callahan, P. J. (1981) *Biochemistry 20*, 7333–7338.

Puskin, J. S., Vistnes, A. I., & Coene, M. T. (1981) *Arch. Biochem. Biophys. 206*, 164–172.

Reed, P. W., & Lardy, H. A. (1972) *J. Biol. Chem. 247*, 6970–6977.

Schick, M. J. (1963) *J. Phys. Chem. 67*, 1796–1799.

Spencer, R. D., & Weber, G. (1969) *Ann. N.Y. Acad. Sci. 158*, 361–376.

Spencer, R. D., & Weber, G. (1970) *J. Chem. Phys. 52*, 1654–1663.

Taylor, R. W., Kauffman, R. F., & Pfeiffer, D. R. (1982) in *The Polyether Antibiotics: Carboxylic Acid Ionophores* (Westly, J. W., Ed.) Vol. 1, pp 103–184, Marcel Dekker, New York.

Van Blitterswijk, W. J., Van Hoeven, R. P., & Van Der Meer, B. W. (1981) *Biochim. Biophys. Acta 644*, 323–332.

Weber, G. (1981) *J. Phys. Chem. 85*, 949–953.